

# Effect of molecular concentrations in tissue-simulating phantoms on images obtained using diffuse reflectance polarimetry

Mehrübe Mehrübeoğlu and Nasser Kehtarnavaz

*Department of Electrical Engineering, Texas A&M University, College Station,  
Texas 77843-3128 USA*

*mehrube@ee.tamu.edu, kehtar@image.tamu.edu*

Sohi Rastegar and Lihong V. Wang

*Biomedical Engineering Program, Texas A&M University, College Station,  
Texas 77843-3120 USA*

*rastegar@tamu.edu, LWang@tamu.edu*

**Abstract:** We have investigated the possibility of using diffuse reflectance polarimetry to detect changes caused by different molecular compounds and concentrations in tissue-simulating phantoms. The effects of glucose,  $\beta$ -alanine and l-lysine at different concentrations in turbid media have been investigated separately. This approach is based on the effect of optical properties on the polarization state of light. The results show that this method has potential for determining changes in molecular concentrations in highly scattering biological media from polarization images.

©1998 Optical Society of America

OCIS codes: (290.0290) Scattering; (100.0100) Imaging systems

---

## References and links

1. R. Farrighetti, ed., *The World Almanac and Book of Facts 1997*, (World Almanac Books, and K-III Reference Corporation, NJ 1996).
2. E. Sevick-Muraca and D. Beneron, eds., *Biomedical Optical Spectroscopy and Diagnostics*, Vol. **3** of OSA Trends in Optics and Photonics (Optical Society of America, Washington, D.C., 1996).
3. M. Kohl and M. Cope, Matthias Essenpreis and Dirk Böcker, "Influence of Glucose Concentration on Light Scattering In Tissue-Simulating Phantoms," *Opt. Lett.* **19**, 2170-72 (1994).
4. J. S. Maier, S. A. Walker, S. Fantini, M. M. A. Franceschini, and E. Gratton, "Possible Correlation Between Blood Glucose Concentration and the Reduced Scattering Coefficient of Tissues in the Near Infrared," *Opt. Lett.* **19**, 2062-64 (1994).
5. J. T. Bruulsema, J. E. Hayward, T. J. Farrell, and M. S. Patterson, L. Heinemann, M. Berger, T. Koschinsky, J. Sandahl-Christiansen, H. Orskov, M. Essenpreis, G. Schmelzeisen-Redeker, and D. Böcker, "Correlation Between Blood Glucose Concentration in Diabetics and Noninvasively Measured Tissue Optical Scattering Coefficient," *Opt. Lett.* **22**, 190-2 (1997).
6. M. R. Ostermeyer, D. V. Stephens, L. -H. Wang, and S. L. Jacques, "Nearfield polarization effects on light propagation in random media," in *Biomedical Optical Spectroscopy and Diagnostics*, E. Sevick-Muraca and D. Benaron, eds., Trends in Optics and Photonics **3**, 20-25 (1996).
7. S. L. Jacques, M. Ostermeyer, L.-H. Wang, and D. V. Stephens, "Polarized light transmission through skin using video reflectometry: toward optical tomography of superficial tissue layers," in *Lasers and Surgery: Advanced Characterization, Therapeutics, and Systems VI*, R. R. Anderson, ed., Proc. Soc. Photo-Opt. Instrum. Eng. **2671**, 199-210 (1996).
8. A. H. Hielscher, A. A. Eick, J. R. Mourant, J. P. Freyer, and I. J. Bigio, "Biomedical Diagnostic with Diffusely Backscattered Linearly and Circularly Polarized Light," *SPIE* **2976**, 298-305 (1997).

9. B. D. Cameron, M. J. Raković, M. Mehrübeoğlu, G. W. Kattawar, S. Rastegar, L. V. Wang, and G. L. Coté, "Measurement and calculation of the two dimensional backscattering Mueller matrix of a turbid medium," *Opt. Lett.* **23**, 485-487 (1998).
10. A. H. Hielscher, A. A. Eick, J. R. Mourant, D. Shen, J. P. Freyer, and I. J. Bigio, "Diffuse backscattering Mueller matrices of highly scattering media," *Opt. Express* **1**, 441-454 (1997). <http://epubs.osa.org/oearchive/pdf/2826.pdf>
11. A. H. Hielscher, J. R. Mourant, and I. J. Bigio, "Influence of Particle Size and Concentration on the Diffuse Backscattering of Polarized Light from Tissue Phantoms and Biological Cell Suspensions," *Appl. Opt.* **36**, 125-135 (1997).
12. M. Dogariu and T. Asakura, "Polarization Dependent Backscattering Patterns from Weakly Scattering Media," *J. Optics* **24**, 271-278 (1993).
13. S. R. Pal and A. I. Carswell, "Polarization Anisotropy in Lidar Multiple Scattering from Atmospheric Clouds," *Appl. Opt.* **24**, 3464-3471 (1985).
14. S. P. Morgan, M. P. Khong, and M. G. Somekh, "Effects of Polarization State and Scatterer Concentration on Optical Imaging Through Scattering Media," *Appl. Opt.* **36**, 1560-65 (1997).
15. R. Greger and U. Windhorst, eds., *Comprehensive Human Physiology from Cellular Mechanisms to Integration*, Vol. **2** (Springer-Verlag, Berlin, 1996), p. 2328.
16. A. C. Guyton, *Textbook of medical physiology*, 8th ed., (Saunders, Philadelphia, Pennsylvania, 1991).
17. D. R. Lide, ed.-in-chief, *CRC Handbook of Chemistry and Physics*, 79th ed., (CRC Press LLC, Boca Raton, Florida, 1998), p. 3-12,8-64.
18. J. G. Grasselli and W. M. Ritchey, eds., *CRC Atlas of Spectral Data and Physical Constants for Organic Compounds*, Vol. **III** (CRC Press, Inc., Cleveland, Ohio, 1975).
19. H. J. van Staveren, C. J. M. Moes, J. van Marle, S. A. Prahl, and M. J. C. van Gemert, "Light scattering in Intralipid-10% in the wavelength range of 400-1100 nm," *Appl. Opt.* **30**, 4507-14 (1991).
20. H. H. Willard, L. L. Meritt, Jr., and J. A. Dean, *Instrumental Methods of Analysis* (Princeton, New Jersey, 1958), pp.320-3.

## 1. Introduction

Today, diabetes affects a significant number of people in the world [1]. In 1995, diabetes mellitus accounted for 2.6% deaths in the United States, corresponding to 59,085 people. Diabetes was the seventh cause of death in the U.S. in 1995 [1]. The current methods used in monitoring glucose levels in blood usually involve pricking the finger and taking a blood sample for testing. The complications caused by diabetes, and the need to continually monitor blood glucose levels are added reasons for the extensive research today for new and improved methods for detecting glucose in biological tissues. Noninvasive optical methods for detecting and monitoring the disease conditions are of particular interest, and are topics of ongoing research [2].

Kohl *et al.* and Maier *et al.* separately studied the effects of increasing glucose in blood on the light scattering properties using a frequency-domain tissue spectrometer and a CCD spectrophotometer, respectively [3, 4]. Bruulsema *et al.* reported measuring reduced scattering coefficient in blood using spatially resolved diffuse reflectance [5]. Several research groups have used diffuse reflectance polarimetry to study properties of turbid media [6-10]. Hielscher *et al.* documented the dependence of polarization patterns on the size and concentration of the scatterers in the medium [11]. Dogariu and Asakura reported studies on polarization patterns obtained from weakly scattering media [12]. In an earlier study, results on polarization anisotropy in multiple scattering regime were reported [13].

In this study, we have investigated the possibility of using diffuse reflectance polarimetry for detecting changing glucose and other molecular concentrations ( $\beta$ -alanine, and l-lysine) in highly scattering tissue-simulating media. These molecular compounds are optically transparent but affect the optical properties of the media. There are two main possible mechanisms that affect the optical properties of the media under study. The first mechanism is a change of the scattering coefficient brought about by the change

of the refractive index of the interstitial fluid due to the addition of different molecules [4]. The second mechanism, which could affect the optical properties, is the optical activity of the added molecules, which causes rotation of the optical polarization. Optical activity is characterized by the chirality of the molecules. A third possible mechanism is molecular interactions within the turbid medium. The diffuse reflectance polarimetry relies on the fact that the polarization of light is affected by the overall optical properties of the medium on which the light is incident [5, 8, 11, 14].

In this study, the changes in polarization pattern images were investigated when different organic materials, namely, glucose (D-(+)-glucose, or dextrose),  $\beta$ -alanine and l-lysine were added in different concentrations to the turbid media. l-lysine and  $\beta$ -alanine are amino acids found only in trace amounts in the body. The average levels of alanine and lysine found in plasma are 420  $\mu\text{mol/l}$  (3.7418 mg/dl) and 200  $\mu\text{mol/l}$  (2.9238 mg/dl), respectively [15]. On the other hand, blood glucose levels vary between 80 and 160 mg/dl in healthy adults but can rise up to 600 mg/dl in diabetic patients [16]. With the primary interest in glucose sensing, l-lysine was chosen due to the fact that it is an optically active, or rather chiral molecule, like glucose.  $\beta$ -alanine is optically inactive, and was chosen for the purpose of comparison among polarization patterns to determine whether the pattern changes were due to optical activity or scattering effect. The index of refraction for D-glucose (0.5% mass) and  $\beta$ -alanine can be found in literature as 1.337 and 1.444 [17], respectively. The specific rotation for l-lysine and D-glucose used in our experiments are cited as 15.29 and 52.7  $^{\circ} \text{ dm}^{-1} (\text{g/dl})^{-1}$  [18].

In diffuse reflectance polarimetry adopted in our experiments, linearly polarized laser light of 1.5 mm diameter was shone onto the surface of the phantoms, and the images of the polarization patterns formed around the area of light incidence were acquired using a CCD camera with a plane polarizer in front of the camera. Here, it is shown that polarization patterns can be affected by the addition of relatively low concentrations of molecules to a highly scattering medium. By adding different concentrations of molecules, we intended to simulate the changes in molecular compound concentrations in interstitial fluid that are possible to occur in actual biological tissues under undesirable disease conditions. Our goal has been to correlate the changes of the polarization patterns with the concentration of the added molecular compounds.

## 2. Materials and methods

Figure 1 illustrates the experimental setup. The light source used was a 594 nm HeNe laser (Uniphase, model 1677, 4mW) with a spot diameter of 1.5 mm, and was normally incident on the phantom. A prism plane polarizer (Newport, LOGTO4AR.14) was used in front of the laser to linearly polarize the incident beam. The diffusely reflected light from the phantom surface went through a second prism plane polarizer (Newport, LOGTO4AR.14) adjusted 90 $^{\circ}$  with respect to the first polarizer, which acted as the analyzer. The 90 $^{\circ}$  orientation of the second polarizer allowed imaging the diffusely reflected light in perpendicular polarization mode. Polarization patterns are formed after the light passes through this second polarizer.

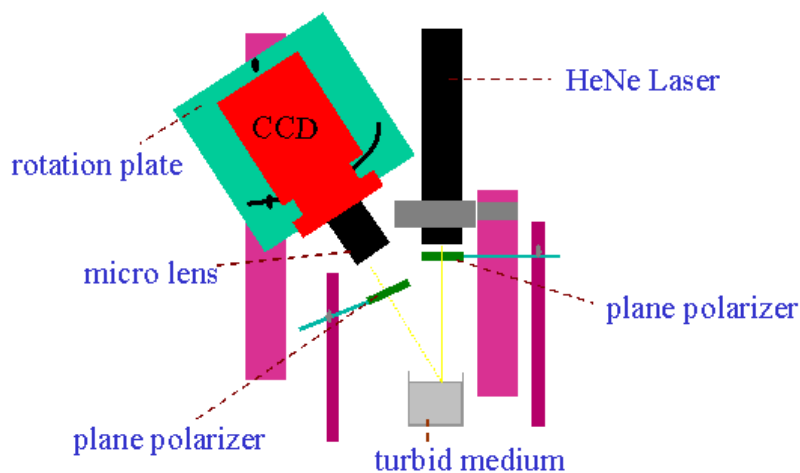


Fig. 1. Experimental system setup for imaging the polarization patterns of the turbid medium using a laser light source, two polarizers, a micro lens, and a CCD camera/detector.

These polarization patterns were collected by a Nikon micro lens attached to an 18-bit CCD camera/detector (EG&G PARC, model 1515P). The CCD camera had a photodetector chip area of  $512 \times 512$  pixels with each pixel area being  $19 \times 19 \mu\text{m}^2$ . The image was focused onto the CCD array by adjusting the focal length of the micro lens and by changing the height of the surface of the phantom to the appropriate focal plane. The camera was held at  $18^\circ$  to the direction of the incident laser beam by an aluminum plate which allowed variable degrees of rotation of the camera. To obtain symmetric images, the camera should be located directly above the point of incidence, or at  $0^\circ$  to the surface normal. However, due to the physical dimensions of the CCD and laser,  $18^\circ$  was the lowest angle that the camera could be adjusted in the system. The CCD camera/detector system was connected to a personal computer for camera control and data acquisition. Image acquisition was achieved via the OMA controller board (EG&G, Model 1564) and WinView Software. All the experiments were performed under dark room conditions. Background images were collected with the laser light off, and subtracted from each of the actual images obtained from the phantom with the laser turned on. The average of twenty-five consecutive images was taken and stored as the final image for each sample to minimize possible laser fluctuation and other system noise effects.

We prepared a liquid phantom with known optical properties (reduced scattering coefficient,  $\mu'_s$ , and absorption coefficient,  $\mu_a$ ) similar to those of biological tissue. The phantom consisted of intralipid suspension and trypan blue dye diluted in distilled water [19], where the intralipid was used as scatterers and trypan blue dye as absorbers. The optical properties of the phantom were  $\mu'_s = 10 \text{ cm}^{-1}$  and  $\mu_a = 0.1 \text{ cm}^{-1}$  obtained from a mixture of 500 ml of distilled water, 165  $\mu\text{l}$  of trypan blue dye, and 14.3 ml of 20% intralipid suspension.

Glucose,  $\beta$ -alanine and l-lysine were added to separate phantom solutions. Each phantom solution was imaged with compound concentration levels of 241, 310, 379, 448, 517, 1207, 2586 and 3965 mg/dl. The lower concentration levels were chosen for their closeness to the actual blood glucose levels of diabetic patients. The concentration range was chosen to test the sensitivity of the system to the amount of added molecular compounds. The experiments were repeated with the same concentrations of  $\beta$ -alanine and l-lysine.

### 3. Results and analysis

For data analysis, first, the raw polarization patterns of images for each concentration were studied. The analyzed image corresponded to a 151X151 pixel area, or an actual imaged area of 9.44X9.44 mm<sup>2</sup>, which sufficiently included the area of the polarization patterns. Outside the central 151X151 pixel image area, the pixel intensity was too low to contribute to quantitative analysis results. The radius of the pattern is approximately two or three transport mean free paths of the medium, where the transport mean free path of the phantom was calculated to be 0.099 cm based on its definition given by  $1/(\mu'_s + \mu_a)$ . Beyond the pattern, the polarization image had no visually distinct features because scattering had randomized the polarization of light. As expected, because the added molecular compound (glucose,  $\beta$ -alanine, l-lysine) quantities were relatively small, no visually noticeable variations among different concentrations and compounds in liquid phantoms could be observed from these raw images (Fig. 2).

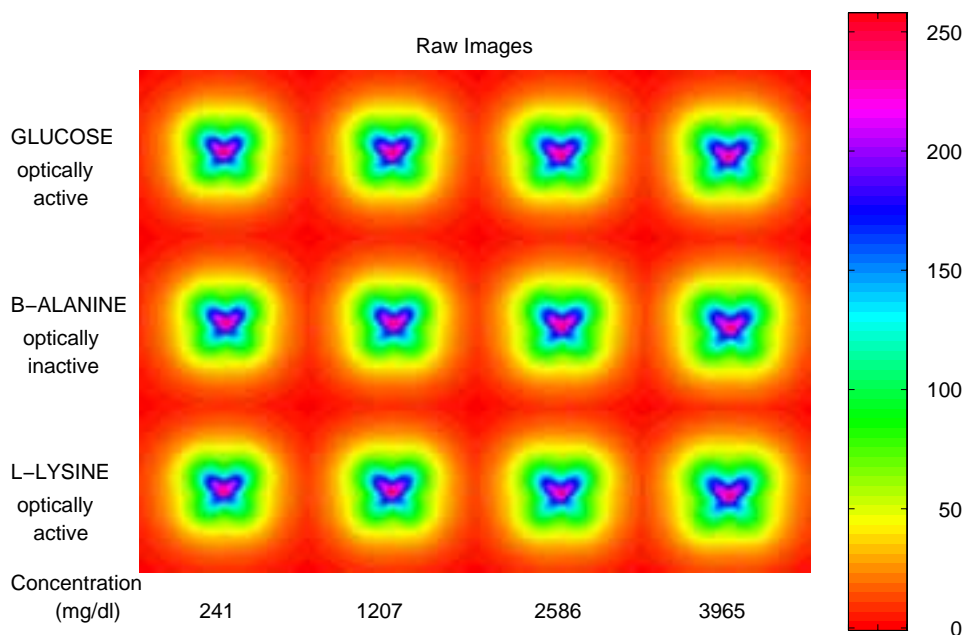


Fig. 2. Sample raw images as obtained by the CCD camera/detector system for glucose,  $\beta$ -alanine and l-lysine. Each row depicts images of increasing concentrations from left to right for the corresponding compound. The asymmetry about the horizontal axis through the center of each row is due to the 18° tilt of the CCD camera and lens system. The spot of laser incidence can be noted in the center of the butterfly patterns.

To extract the small changes brought about by the added small compound amounts, the difference patterns between the images were investigated. In each class (glucose,  $\beta$ -alanine, l-lysine), the image pertaining to the lowest added compound concentration (241 mg/dl) was taken as the reference medium, and subtracted from all the rest of the images to obtain the difference images. The value of 241 mg/dl was chosen as a reference to better represent changes with respect to physiological glucose levels. Before taking the difference images, each individual image was first normalized between the values of 0 and 255 to eliminate the sensitivity to possible laser intensity fluctuations. The difference images were calculated as in Eq. (1),

$$I_d = I_c - I_r \quad (1)$$

where  $I_d$  is the intensity difference image,  $I_c$  is the normalized image of the phantom solution with different concentrations of the added compound, and  $I_r$  is the normalized reference, or the image corresponding to the lowest 241 mg/dl compound concentration.

Figure 3 depicts a set of difference images obtained from the normalized images of glucose,  $\beta$ -alanine and l-lysine in the phantom solution for the covered range of concentrations. As can be seen in Figure 3, there is a distinct pattern intensity change among the highest concentration difference images ( $I_c = 517, 1207, 2586, 3966$  mg/dl, or  $I_d = 276, 966, 2345, 3725$  mg/dl) for all the added compounds in the phantom solutions. The pattern changes become more prominent as the difference between the concentrations increases. The difference images for concentration levels from 310 to 448 mg/dl are not shown. Qualitatively, these images suggest that concentration differences of 966 mg/dl and higher can be detected under the tested conditions for all the mentioned molecular compounds.

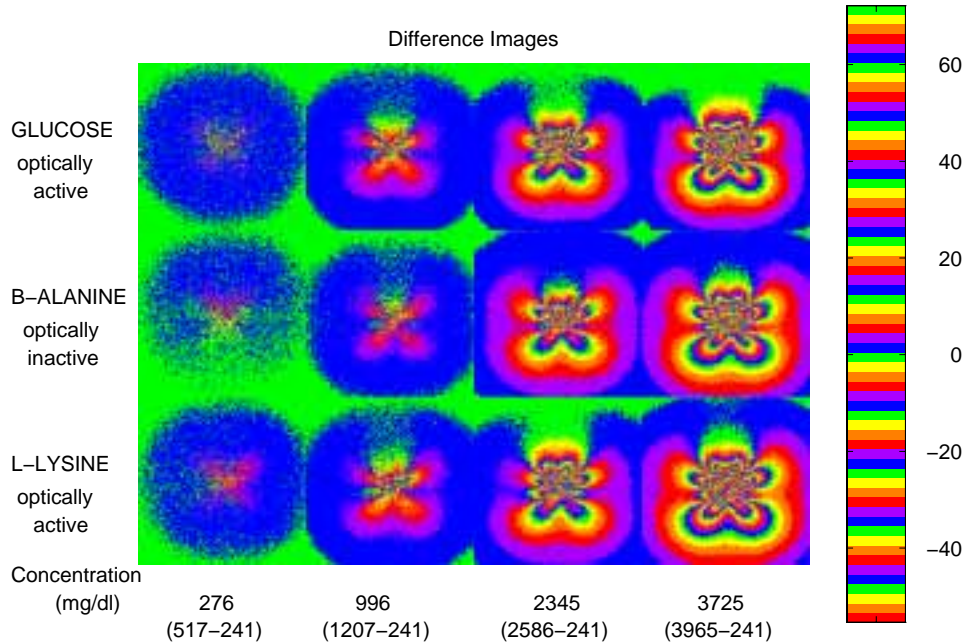


Fig. 3. Difference images within each compound (glucose,  $\beta$ -alanine, l-lysine) with respect to the corresponding image for lowest concentration (241 mg/dl). Each row depicts difference images of increasing concentration from left to right for the compound labeled on the left of each row.

The same observations can be made from the analysis of ratio images when each image was divided by  $I_r$ . Figure 4 shows the ratio images for the same data set.

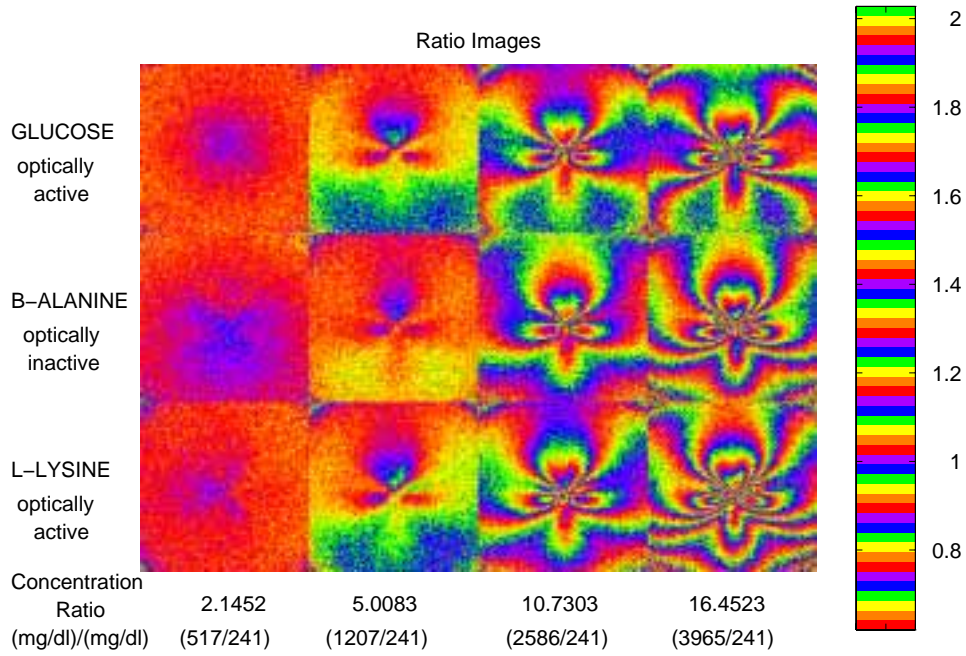


Fig. 4. Ratio images within each compound (glucose,  $\beta$ -alanine, l-lysine) with respect to the corresponding image for lowest concentration. Each row depicts images of increasing concentration ratio from left to right for the compound labeled on the left of each row.

To quantify the changes in these patterns, the correlation (*corr*) between different raw images and different difference images were calculated. For the correlation calculations, the absolute intensity values were used to eliminate negative correlation values. In addition, the mean-square difference (MSD) and root mean-square difference (RMSD) were determined for the raw images. The MSD and RMSD, separately, are similar for raw and difference images, as can be deduced from the equations that follow. The correlation, MSD and RMSD were calculated with respect to the lowest concentration image in the corresponding classes. The correlation and mean-square difference between two images are found by Eq. (2) and Eq. (3), respectively,

$$corr(n, l) = \frac{\sum_{i=1}^{151} \sum_{j=1}^{151} (img_n(i, j) \times img_l(i, j))}{\sqrt{\sum_{i=1}^{151} \sum_{j=1}^{151} (img_n(i, j) \times img_n(i, j)) \times \sum_{i=1}^{151} \sum_{j=1}^{151} (img_l(i, j) \times img_l(i, j))}} \quad (2)$$

$$MSD(n, l) = \frac{1}{(151)^2} \sum_{i=1}^{151} \sum_{j=1}^{151} (img_n(i, j) - img_l(i, j))^2 \quad (3)$$

where  $l$  indicates the medium with the lowest concentration,  $n$  indicates all other media with higher concentrations,  $img_l$  is the image pertaining to the lowest concentration,  $img_n$  represents an image of a higher concentration level, and  $i$  and  $j$  are Cartesian coordinates of the pixels in each image. The RMSD is calculated from MSD as in Eq. (4).

$$RMSD(n, l) = \sqrt{MSD(n, l)} \quad (4)$$

The correlation, MSD and RMSD analyses used takes advantage of the entire data points within the 2D image. This reduces possible noise effects in calculations by smoothing out or averaging all the information within an image.

Figures 5 and 6 show the correlation plots among the raw and difference images. MSD and RMSD plots are presented in Figures 7 and 8.

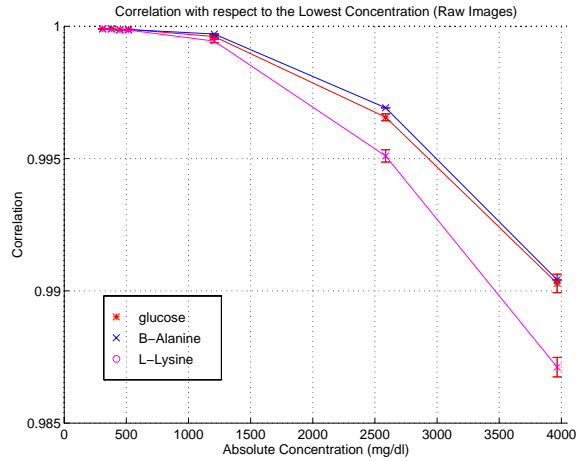


Fig. 5. Correlation between raw images. Correlation is plotted for each compound, namely, glucose,  $\beta$ -alanine and l-lysine, with respect to the lowest concentration in each class, against increasing concentration (mg/dl).

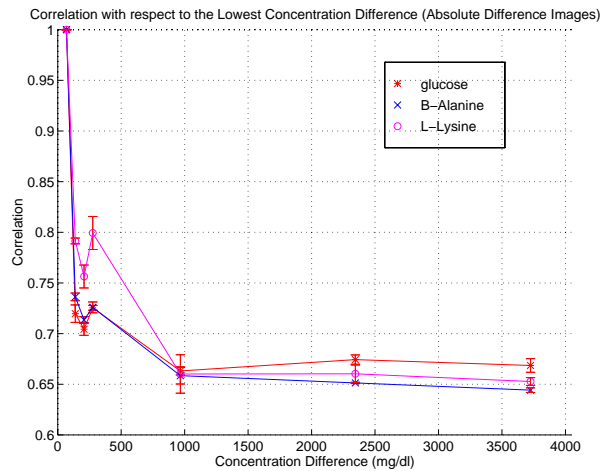


Fig. 6. Correlation between difference images. The absolute value of the intensity of the difference images was used to obtain positive correlation values. Correlation is plotted for each compound (glucose,  $\beta$ -alanine and l-lysine) against increasing concentration difference (difference relative to the 241 mg/dl images).



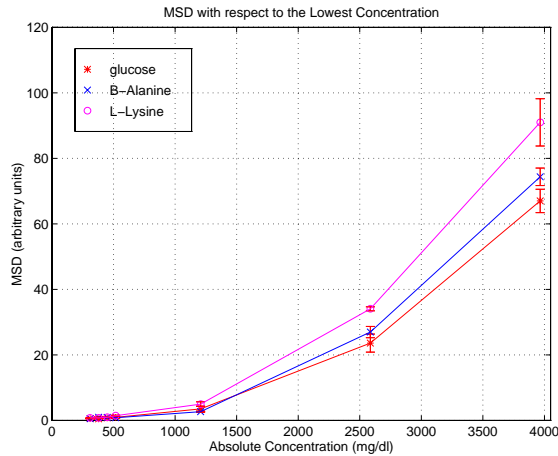


Fig. 7. Mean-Square Difference for all molecular compounds with respect to the lowest concentration (241 mg/dl) image.

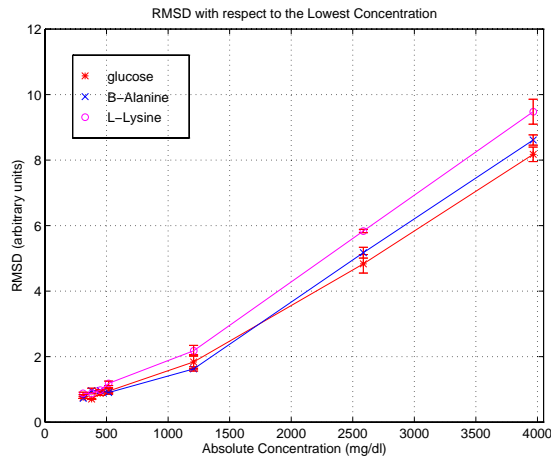


Fig. 8. Root Mean-Square Difference for all molecular compounds with respect to the lowest concentration (241 mg/dl) image. Of particular importance is the linear change of the polarization patterns with respect to increasing glucose concentration.

The correlation and MSD plots show that currently, it is possible to differentiate between concentration differences larger than 276 (517-241) mg/dl both in the case of optically active and inactive molecules. Figure 5 shows a distinct decrease in the correlation with respect to the lowest concentration image as the concentration increases beyond 517 mg/dl. Similarly, in Figure 7, the MSD increases markedly beyond concentration levels of 517 mg/dl, suggesting the separability of patterns above this concentration level. Figure 6 shows similar trends for the higher concentration difference levels suggesting noise in the correlation among low concentration difference images. The results hold true for all glucose,  $\beta$ -alanine and l-lysine experiments. Figure 8 is showing an approximately linear dependence of the RMSD value with respect to the added glucose concentration.

Correlation for ratio images is similar to those of raw images. MSD and RMSD results for ratio images follow the same trend as those results for raw and difference images.

#### 4. Discussion and conclusions

As mentioned before, when the organic substances are added into the phantom, two main possible factors could alter the images of the diffuse reflectance polarimetry. The first factor is the variation in the concentration of the added substance in the interstitial fluid, which leads to a change in the index of refraction of the interstitial fluid. Because the scattering coefficient depends on the relative index of refraction between the intralipid scatterers and the interstitial fluid, the change in the index of refraction of the interstitial fluid alters the scattering coefficient of the phantom. The second factor is the optical activity of the added substances. Glucose and l-lysine are optically active molecules, which means that they rotate the polarized light upon interaction with them. On the other hand,  $\beta$ -alanine is an optically inactive molecule, which means  $\beta$ -alanine does not cause changes in the angle of polarization of the light incident upon it.

The fact that similar trends in polarization patterns were observed both in the case of optically active and inactive molecules suggests that the changes in polarization patterns due to the added substances are dominated by the changes in the refractive index of the interstitial fluid. This is further supported by the linear relation between the concentration of glucose, and refractive index, and the former and reduced scattering coefficient. Figure 9(a) shows how the refractive index of water is affected by the addition of glucose [4]. Figure 9(b) shows the effect of glucose concentration on the reduced scattering coefficient of the scattering medium with an initial  $\mu'_s$  of  $10 \text{ cm}^{-1}$  as in our experiments [4]. These graphs were calculated assuming a refractive index of 1.46 for the scatterers, and 1.325 for the water [4, 19]. Figure 9(b) was calculated using Rayleigh-Gans theory [4] as in Eq. (5),

$$\mu'_s = K \frac{(n_1 - n_0)}{n_0} \quad (5)$$

where  $n_1=1.46$ ,  $n_0=1.325$ , and the proportionality factor,  $K=963 \text{ cm}^{-1}$ .

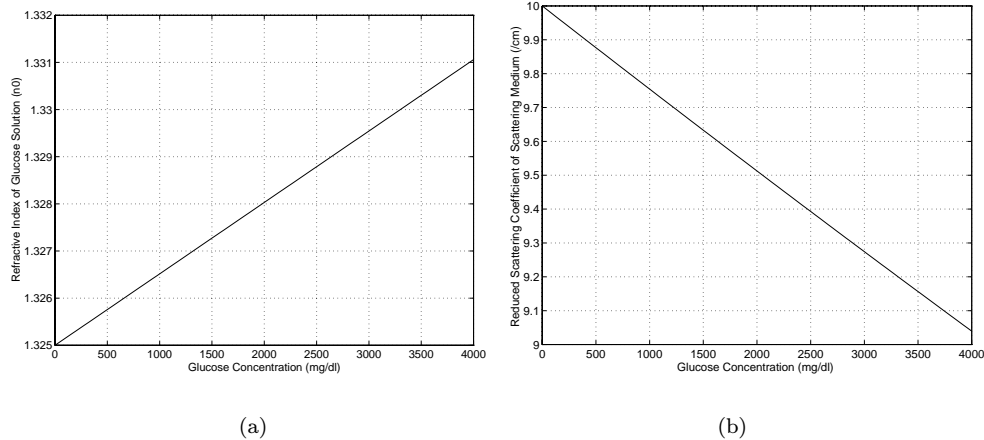


Fig. 9. Effect of Glucose concentration on the refractive index of water (a) and the reduced scattering coefficient of turbid medium (b). A linear relation can be observed between added glucose and refractive index of water. The same is true for added glucose and reduced scattering coefficient of turbid medium.

The optical activity does not contribute as significantly to the polarization patterns at the concentration levels of our experiments. The optical activity of glucose

causes minute rotation of light because of the short path length of light contributing to the polarization patterns. Glucose has a specific rotation of  $52.5^\circ \text{ dm}^{-1} (\text{g/dl})^{-1}$  at 589 nm incident wavelength [20]. In more familiar units, this translates into  $52.5 \times 10^{-7}$  degrees of rotation of the polarization vector for each mm of pattern length and for each added glucose concentration of 1 mg/dl.

The rotation caused by glucose can, therefore, be estimated using the following formula,

$$\phi = (5.25 \times 10^{-7})lc \quad (6)$$

where  $\phi$  is the rotation of the incident polarization vector caused by glucose, in degrees,  $l$  is the polarization pattern radius in mm, and  $c$  is the added glucose concentration in mg/dl.

It is important to point out that the reason why, in our experiments, the pattern radius, and not the pathlength traveled by photons, can be used to estimate the total rotation caused by glucose, is that from the point of incidence to the outer edge of the pattern, light travels a horizontal distance that is equal to the pattern radius while it makes a round trip vertically. Only the horizontal propagation contributes to the rotation of polarization; and the round trip has a zero net rotation because the upward and downward propagations cancel each other's contributions to the rotation. Therefore, the rotation is related to the pattern radius rather than the pathlength.

For a pattern length of about 5.8 mm with a pattern radius of 2.9 mm, which is representative of the collected images in our experiments (Fig. 2), at the low glucose concentrations between 241 and 517 mg/dl, the rotation is between 0.367 and 0.787 milli degrees. Between concentration levels of 1207 and 3966 mg/dl, rotation increases to between 1.838 and 6.038 milli degrees. The optical rotation caused by l-lysine can also be calculated in a similar fashion. The calculated rotation values hint minimal contribution to the cross-polarization patterns by the polarization vector rotated by glucose.

These results may suggest that the rotation induced by glucose is minute at the tested concentration levels, and the main effect on the patterns are due to changes in the refractive index, hence the reduced scattering coefficient.

Molecular interactions between the host medium and added compounds are also possible and require further investigations for their possible effect on polarization patterns.

Overall these results show that the method of diffuse reflectance polarimetry can be used to identify variations in concentrations of different compounds in turbid media. This is a novel approach in determining concentration changes of interstitial fluids. These results are very encouraging.

The concentration levels tested for  $\beta$ -alanine and l-lysine are much higher than what is found in the body. This method may not be adequate for biological detection of these two substances. However, within the tested concentration range,  $\beta$ -alanine and l-lysine provide a good comparison for the behavior of different molecules in turbid media. From the results of our experiments, the trend in the change of the refractive index with respect to increasing concentration caused by the three compounds are comparable.

Further studies include detecting concentration differences at physiologic levels for glucose, and developing elaborate feature extraction techniques to quantify and correlate small pattern changes to molecular concentrations and optical property changes at lower molecular levels. The following stages of this research involve multiple studies on data to be acquired from actual biological tissues, and the development of an algorithm for automatic determination of compound levels in tissues, which can be used

clinically for diagnoses and monitoring.

### **Acknowledgements**

We thank A. Hebert, K. Wyly and J. Keller for their assistance during the experiments. This project is sponsored in part by the Office of VP for Research at Texas A&M University, the Whitaker Foundation, and the National Institute of Health grants R29 CA68562 & R01 CA71980.